ALEPH 89-21
Add. distr. TPC ITC 89-1
R. Forty
7.2.1989

# Assembly of the ITC and TPC

R.W. Forty
*Imperial College, London*

**Abstract**

**The technique used for the insertion of the ITC into the TPC is described. The procedure was performed successfully, and the results of survey measurements are given indicating that the chambers were well aligned.**

## 1 Introduction

The ITC takes the form of a cylinder of 600 cm diameter and 2 m length. It is supported within the TPC by support tubes of the same diameter, that extend the length of the cylinder to 4·6 m, to match that of the TPC. The TPC, on the other hand, has a cylindrical bore that the ITC is intended to fit into, of diameter equal to that of the ITC plus about 8 mm clearance. The inner wall of the TPC is a thin skin of low-mass material to minimize multiple scattering, and is therefore delicate. The problem discussed in this note is the insertion of the 4·6 m length of the ITC, extended further by attached vacuum pump assemblies, into this bore without touching the TPC inner wall.

The support tubes of the ITC end in flanges that are fitted with 4 survey targets, at each end, as described in Ref. 1. Once in position inside the TPC, the support flanges rest on two fibre-glass faced pads at each end, attached to the TPC endplates,

that define the relative alignment of the two detectors. The correct positioning of these pads is decided before insertion of the chamber using a target ring system. Then after insertion the position of the chamber is determined using the survey targets. These procedures are also described below.

# 2 Preparation

Two target rings are used, one for each end of the chamber, each with a cross-hair of 30 $\mu$m wire that had been previously set to lie on the true ITC axis [1]. During handling of the $B$-end ring the vertical cross-hair wire was broken, but as its position is defined by the wire mounting arrangement on the ring, a new wire was easily installed. The rings were set up on the support pads at each end of the TPC and the position of the cross-hair determined by surveying.

The aim is to align the cross-hair to the centre of the TPC endface, at each end. This centre is determined using survey targets on the TPC, of which there are various types: for each sector there is a survey target on its centre-line, towards its outer edge, in the form of a brass disk with a central hole (of $\sim 500\,\mu$m diameter). The position of these is illustrated in Fig. 1 (a) for the $A$-end and (b) for the $B$-end, shown looking at the endface from outside the TPC in both cases, where the sectors are labelled following Ref. 2. There are also second targets on each sector towards the inner edge, of which only a few were used (labelled with a prime in Fig. 1). Finally there are 'mechanical' survey targets, attached to the sector support structure, which take the form of pointed rods projecting from each endface. Also shown in Fig. 1 is the coordinate system used to describe each end: $x$ is horizontal and $y$ vertical. The $x$-axis and the TPC endface are not parallel, however, and their relative angle differs at each end—this led to some complications, as will be seen.

The raw coordinates of the TPC sector survey targets (relative to an arbitary origin) are given in Tables 1 and 2 for the two ends [3]. Not all the targets are used, as some were not visible to the surveyors. To determine the centre of each endface in the transverse ($x$, $y$) plane, circles were fit through these coordinates. As there are three types of sector—inner, and two outer—with differing nominal radii for their targets, three separate circle fits were performed, labelled $a$, $b$ and $c$ in the tables.

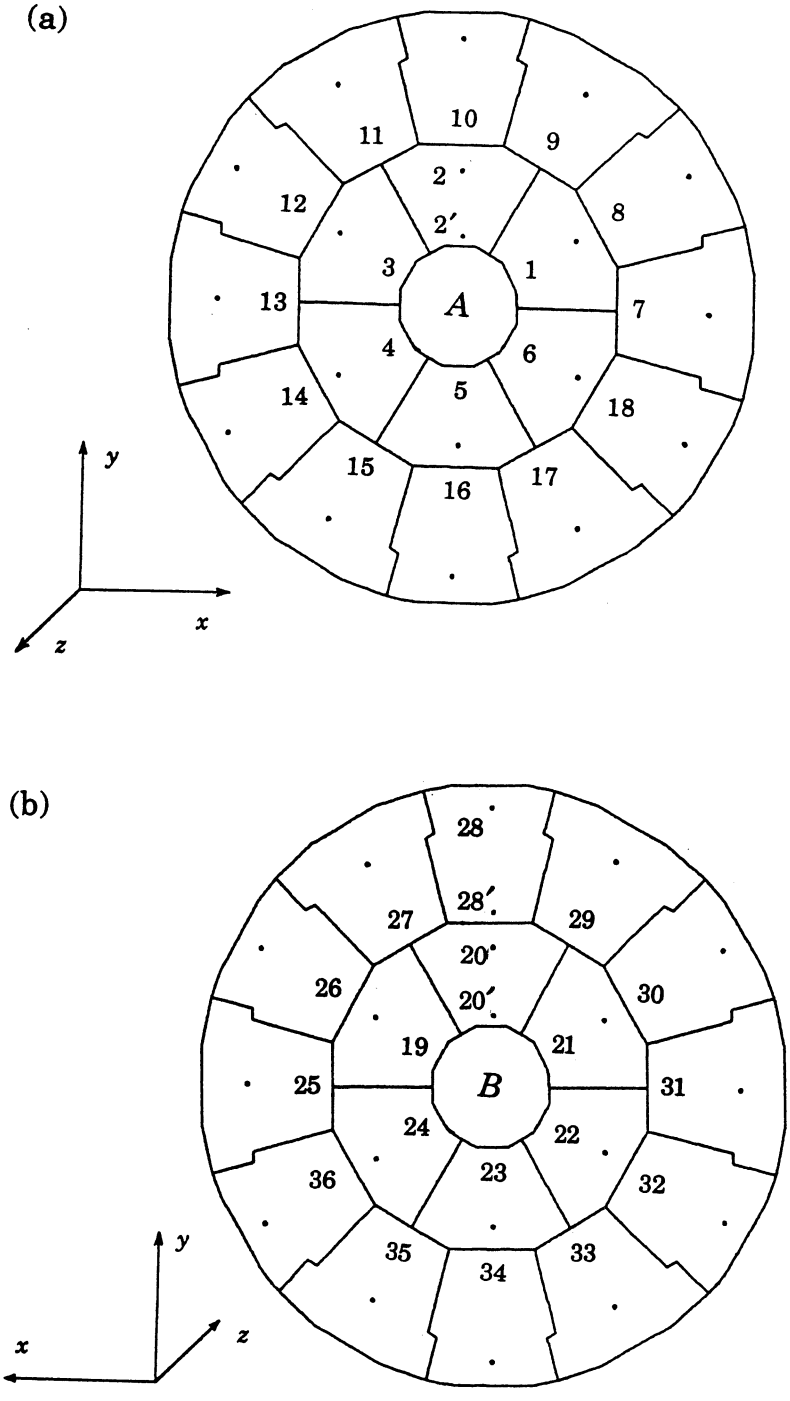


**Figure 1** *The TPC survey targets*

| Sector | $x_{raw}$ [m] | $y_{raw}$ [m] | $-z_{raw}$ [m] | Fit | $\Delta R$ [$\mu$m] |
|---|---|---|---|---|---|
| 2 | 11·93739 | 50·00745 | 12·20463 | *a* | 30 |
| 4 | 11·27521 | 48·86376 | 12·21941 | *a* | −40 |
| 5 | 11·93567 | 48·48133 | 12·20459 | *a* | 60 |
| 6 | 12·59676 | 48·86214 | 12·18935 | *a* | −40 |
| 9 | 12·68559 | 50·53801 | 12·18758 | *b* | 60 |
| 10 | 11·93831 | 50·80317 | 12·20485 | *c* | −10 |
| 11 | 11·19097 | 50·53954 | 12·22186 | *b* | −70 |
| 13 | 10·44206 | 49·24614 | 12·23853 | *b* | 20 |
| 14 | 10·58585 | 48·46652 | 12·23504 | *c* | 10 |
| 15 | 11·18773 | 47·95071 | 12·22106 | *b* | 40 |
| 16 | 11·93444 | 47·68578 | 12·20366 | *c* | −20 |
| 17 | 12·68241 | 47·94878 | 12·18720 | *b* | −50 |
| 18 | 13·28545 | 48·46338 | 12·17360 | *c* | 10 |
| 2′ | 11·93690 | 49·64453 | 12·20512 | | |

**Table 1** *Raw TPC survey target coordinates, A end*

| Sector | $-x_{raw}$ [m] | $y_{raw}$ [m] | $z_{raw}$ [m] | Fit | $\Delta R$ [$\mu$m] |
|---|---|---|---|---|---|
| 19 | 11·03748 | 49·62304 | 13·34752 | *a* | 240 |
| 20 | 11·69807 | 50·00512 | 13·34351 | *a* | −240 |
| 21 | 12·35951 | 49·62451 | 13·33983 | *a* | 40 |
| 22 | 12·36047 | 48·86154 | 13·34020 | *a* | 150 |
| 23 | 11·69979 | 48·47941 | 13·34403 | *a* | −150 |
| 24 | 11·03865 | 48·86011 | 13·34766 | *a* | −50 |
| 25 | 10·20401 | 49·24074 | 13·35289 | *b* | 130 |
| 26 | 10·34784 | 50·02009 | 13·35225 | *c* | 190 |
| 27 | 10·94985 | 50·53590 | 13·34843 | *b* | 30 |
| 28 | 11·69714 | 50·80092 | 13·34386 | *c* | 190 |
| 29 | 12·44485 | 50·53753 | 13·33962 | *b* | −190 |
| 30 | 13·04825 | 50·02332 | 13·33630 | *c* | 90 |
| 31 | 13·19398 | 49·24403 | 13·33567 | *b* | 160 |
| 35 | 10·95289 | 47·94712 | 13·34890 | *b* | −150 |
| 36 | 10·34977 | 48·96150 | 13·35244 | *c* | −100 |
| 20′ | 11·69855 | 49·64214 | 13·34359 | | |
| 28′ | 11·69759 | 50·24096 | 13·34203 | | |

**Table 2** *Raw TPC survey target coordinates, B end*

The results of the circle fits are shown in Tables 3 and 4 for the two ends. As can be seen, the coordinates of the circle centre, $x_0$ and $y_0$, for the three fits at each end agree well, to better than $\sim 200\,\mu$m. A mean centre is calculated, weighting each individual fit by the number of points $N_{pts}$ included in it. The radii $R$ of the fit circles are given in the tables, and are used to determine the radial offset of each of the sector targets from the average value. The offsets are given in Tables 1 and 2, and are illustrated in Fig. 2. As can be seen, they are typically only $\sim 100\,\mu$m. Also shown in Tables 3 and 4 are the results of the fit of a circle to the mechanical survey targets, labelled *d*. This 'mechanical' centre agrees with the results from the sector target fits, although only after a correction for the angular difference between survey $x$-axis and the TPC endface, that will be discussed below.

| Fit | $x_0$ [m] | $y_0$ [m] | $-z_0$ [m] | $R$ [m] | $N_{pts}$ |
|---|---|---|---|---|---|
| *a* | 11·93645 | 49·24441 | | 0·76302 | 4 |
| *b* | 11·93683 | 49·24425 | | 1·49475 | 5 |
| *c* | 11·93655 | 49·24447 | | 1·55871 | 4 |
| Mean | 11·93663 | 49·24437 | 12·20442 | | |
| *d* | 11·9366 | 49·2444 | | 1·4866 | 4 |

**Table 3** *Fit to TPC survey target coordinates, A end*

| Fit | $-x_0$ [m] | $y_0$ [m] | $z_0$ [m] | $R$ [m] | $N_{pts}$ |
|---|---|---|---|---|---|
| *a* | 11·69903 | 49·24231 | | 0·76305 | 6 |
| *b* | 11·69898 | 49·24228 | | 1·49484 | 5 |
| *c* | 11·69903 | 49·24218 | | 1·55894 | 4 |
| Mean | 11·69901 | 49·24226 | 13·34405 | | |
| *d* | 11·6991 | 49·2423 | | 1·4866 | 5 |

**Table 4** *Fit to TPC survey target coordinates, B end*

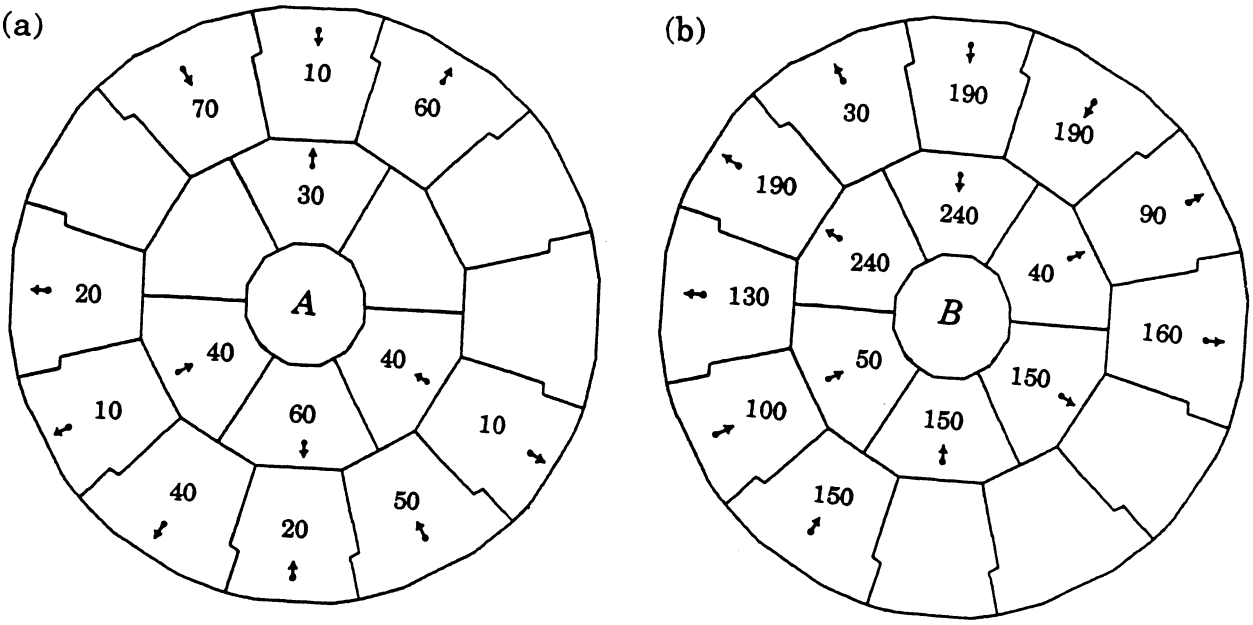


**Figure 2** *The TPC survey target radial offsets [$\mu m$]*

To determine the centre in $z$, the $z$-coordinates of the targets are plotted in Fig. 3 as a function of $x$ (given relative to $x_0$). As can be seen, the points—which come from widely varying $y$-coordinates—all lie on a straight line, indicating that the survey coordinate system is aligned to the TPC in $y$, but is at an angle in $x$. A straight line was fit through the points, of the form

$$z_{raw} = \alpha x + z_0$$

with the result shown superimposed in the figure. This gives

$$\alpha_A = -22{\cdot}75\,\text{mrad}$$
$$\alpha_B = +5{\cdot}90\,\text{mrad} \quad .$$

The values of $z_0$ are shown in Tables 3 and 4. Correcting the raw coordinates of the TPC survey targets so that they are given relative to the calculated centres $(x_0, y_0, z_0)$ leads to the values given in Tables 5 and 6 for the two ends.

(a) *A*-end

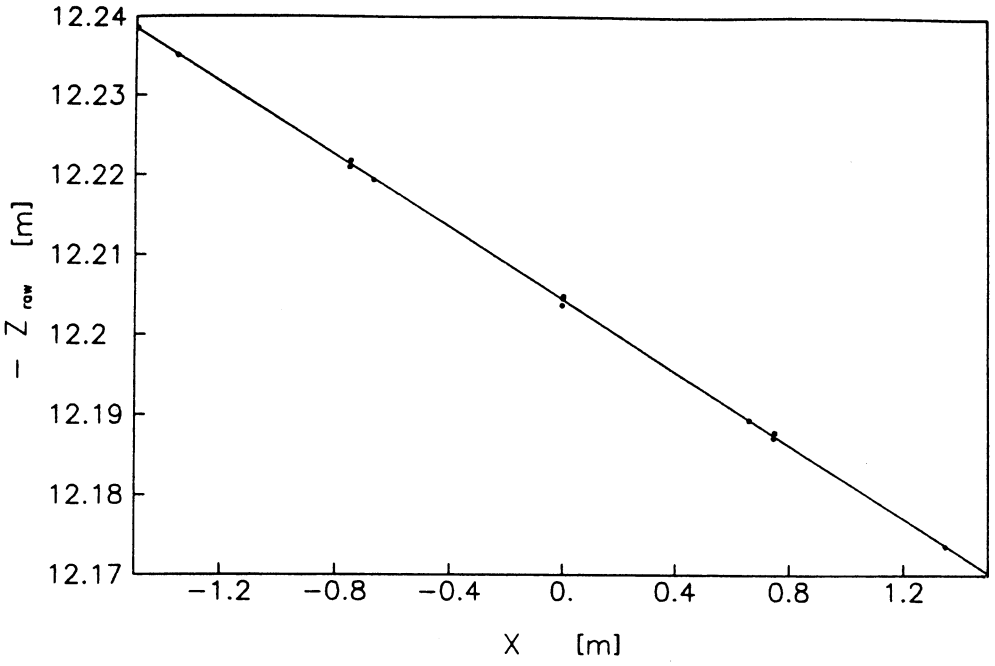


(b) *B*-end

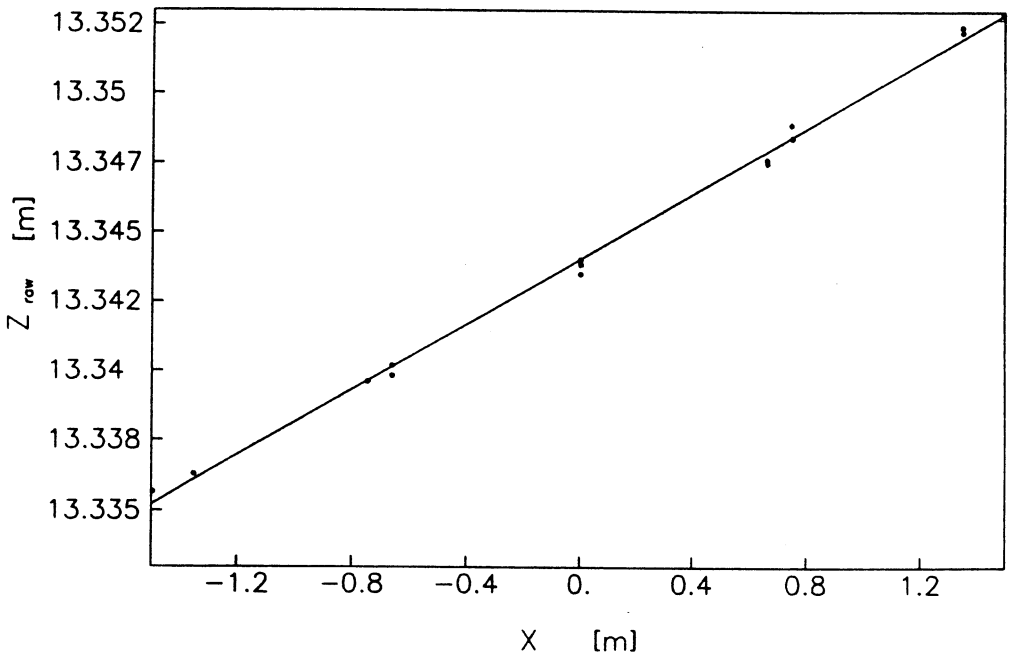


**Figure 3** *The z-coordinate of the TPC survey targets v. x*

| Sector | $x$ [m] | $y$ [m] | $z$ [mm] |
|---|---|---|---|
| 2 | 0·00076 | 0·76308 | −0·21 |
| 4 | −0·66142 | −0·38061 | −14·99 |
| 5 | −0·00096 | −0·76304 | −0·17 |
| 6 | 0·66013 | −0·38223 | 15·07 |
| 9 | 0·74896 | 1·29364 | 16·57 |
| 10 | 0·00168 | 1·55880 | −0·43 |
| 11 | −0·74566 | 1·29517 | −17·44 |
| 13 | −1·49457 | 0·00177 | −34·11 |
| 14 | −1·35078 | −0·77785 | −30·62 |
| 15 | −0·74890 | −1·29366 | −16·64 |
| 16 | −0·00219 | −1·55859 | 0·76 |
| 17 | 0·74551 | −1·29559 | 17·22 |
| 18 | −1·34882 | −0·78099 | 30·82 |
| 2′ | 0·00027 | 0·40016 | −0·70 |

**Table 5** *Corrected TPC survey target coordinates, A end*

| Sector | $x$ [m] | $y$ [m] | $z$ [mm] |
|---|---|---|---|
| 19 | 0·66153 | 0·38078 | 3·47 |
| 20 | 0·00094 | 0·76286 | −0·54 |
| 21 | −0·66050 | 0·38225 | −4·22 |
| 22 | −0·66146 | −0·38072 | −3·85 |
| 23 | −0·00078 | −0·76285 | −0·02 |
| 24 | 0·66036 | −0·38215 | 3·61 |
| 25 | 1·49500 | −0·00152 | 8·84 |
| 26 | 1·35117 | 0·77783 | 8·20 |
| 27 | 0·74916 | 1·29364 | 4·38 |
| 28 | 0·00187 | 1·55866 | −0·19 |
| 29 | −0·74584 | 1·29527 | −4·43 |
| 30 | −1·34924 | 0·78106 | −7·75 |
| 31 | −1·49497 | 0·00177 | −8·38 |
| 35 | 0·74612 | −1·29514 | 4·85 |
| 36 | 1·34924 | −0·78076 | 8·39 |
| 20′ | 0·00046 | 0·39988 | −0·46 |
| 28′ | 0·00142 | 0·99870 | −2·02 |

**Table 6** *Corrected TPC survey target coordinates, B end*

| | A | | | B | | |
|---|---|---|---|---|---|---|
| Survey | $x$ [$\mu$m] | $y$ [$\mu$m] | $z$ [mm] | $x$ [$\mu$m] | $y$ [$\mu$m] | $z$ [mm] |
| 1 | −2040 | 2460 | * | −800 | 2040 | * |
| 2 | 0 | −200 | 56·5 | 70 | −140 | −58·9 |
| 3 | −1160 | 300 | 56·6 | 250 | 140 | −58·9 |

* No value given

**Table 7** *Target ring cross-hair coordinates*

The coordinates of the target ring cross-hairs were then measured. The results [3] are given relative to $(x_0, y_0, z_0)$ in Table 7. To align the cross-hairs to the TPC endface centres, the fibre-glass facings of the support pads were machined down. There was some concern that removal and replacement of the pads might change their position, so this was checked by removing and replacing them without any machining, and remeasuring their position. It was found that the resulting change in position of the cross-hair was $\sim 200\,\mu$m. This rather large change was due to play in the screw threads locating the pads, so a technique of applying pressure to the pads as they were replaced was developed, which reduced the change of position on replacement to $< 50\,\mu$m.

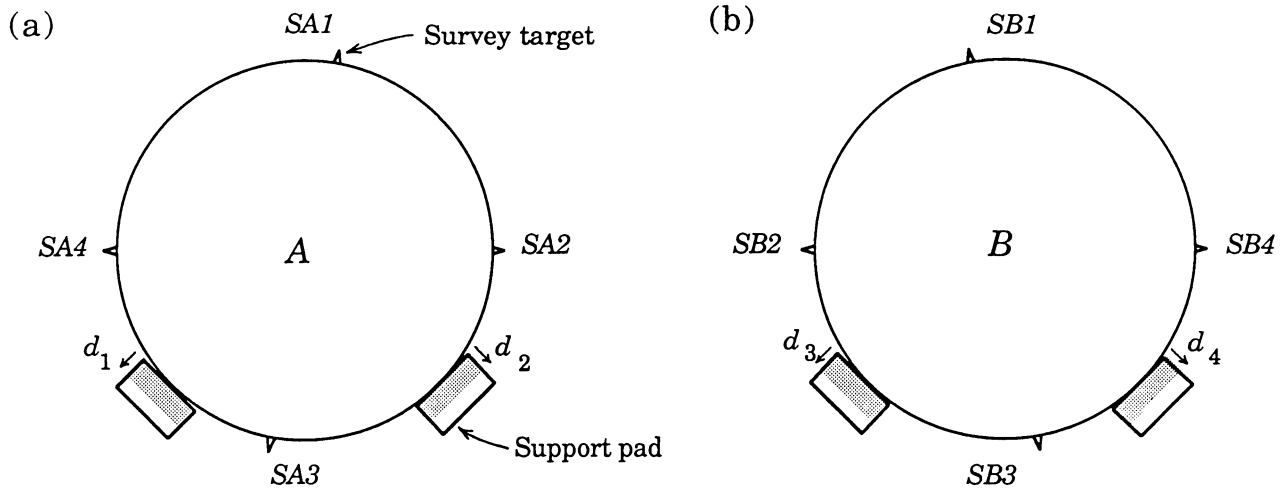


**Figure 4** *The ITC support pads*

The pads are at a 45° angle to the vertical (see Fig. 4). For offsets $\delta x$ and $\delta y$, the amount to be removed from the pads is given by

$$d_1 = \frac{-(\delta x + \delta y)}{\sqrt{2}}$$
$$d_2 = \frac{(\delta x - \delta y)}{\sqrt{2}} \quad ,$$

where $d_1$ and $d_2$ are removed from the left- and right-hand pads at the $A$-end (viewed from outside the TPC), and a similarly calculated $d_3$ and $d_4$ are removed from the left- and right-hand pads at the $B$-end. The first measurement of the cross-hair position is given in row 1 of Table 7. To correct for the offsets seen, the following quantities were machined from the pads:

$$d_1 = 0{\cdot}28\,\text{mm}$$
$$d_2 = 3{\cdot}11\,\text{mm}$$
$$d_3 = 1{\cdot}98\,\text{mm}$$
$$d_4 = 0{\cdot}85\,\text{mm} \quad .$$

The cross-hair position was then remeasured, giving the results shown in row 2 of Table 7, which shows that the cross-hairs now appeared to be well aligned to the endface centres.

At this point it was noticed that the original calculations of the mechanical centres of the TPC endfaces differed substantially from the centres determined using the sector targets. The mechanical centre appeared to be offset at the $A$-end by $\sim 5\,\text{mm}$ to the left, and at the $B$-end by $\sim 1\,\text{mm}$ to the left. It was realized that this offset was not real—it was an effect of the difference in angle between the $x$-axis of the survey coordinate system and the TPC endfaces. Since the mechanical survey targets are in the form of rods projecting from the endface, they lie at a different $z$-coordinate from the sector targets. The angle therefore leads to an apparent offset in $x$. If this effect is taken into account, the centre of the endface measured from the mechanical targets agrees with that from the sector targets, as was shown in Tables 3 and 4 for each end. However, the cross-hairs of the target rings for the ITC alignment are also at a different $z$-coordinate from the TPC endplate centres, as seen in Table 7. There is therefore also an apparent offset introduced here, illustrated in Fig. 5. The offset is in $x$, and is given by

$$\Delta x = d \sin\alpha \quad .$$

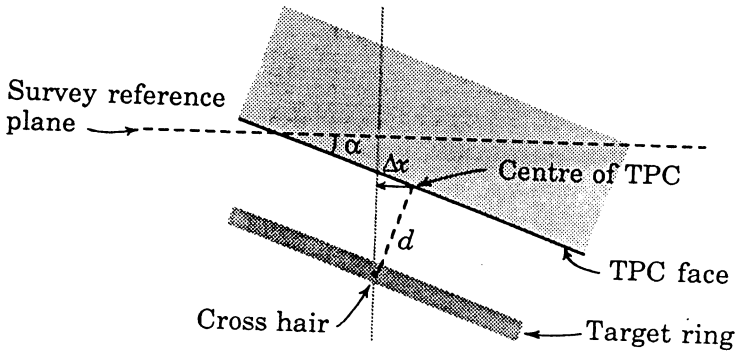


**Figure 5** *Effect of the angular displacement of the survey axis*

This had not been allowed for in the pad adjustments described above. Using the angles determined earlier, we find

$$\Delta x_A = -1290\,\mu\text{m}$$

$$\Delta x_B = +350\,\mu\text{m} \quad .$$

To account for these offsets, and to adjust for the remaining offsets from the previous attempt, the pads were machined a second time, with changes:

$$d_1 = +0{\cdot}77\,\text{mm}$$

$$d_2 = -1{\cdot}05\,\text{mm}$$

$$d_3 = +0{\cdot}04\,\text{mm}$$

$$d_4 = -0{\cdot}32\,\text{mm} \quad .$$

The negative values indicate an increase in the pads thickness. This was achieved by machining the pad down $\sim 0{\cdot}5\,\text{mm}$ and then attaching a thin layer of fibre-glass with epoxy adhesive, which was then machined down to give the required thickness.

The final position of the target ring cross-hairs are given in row 3 of Table 7. Bearing in mind the offsets $\Delta x$ given above, this leads to the relative alignment shown in Fig. 6. The errors on these positions are estimated as $\pm 200\,\mu\text{m}$ [3].

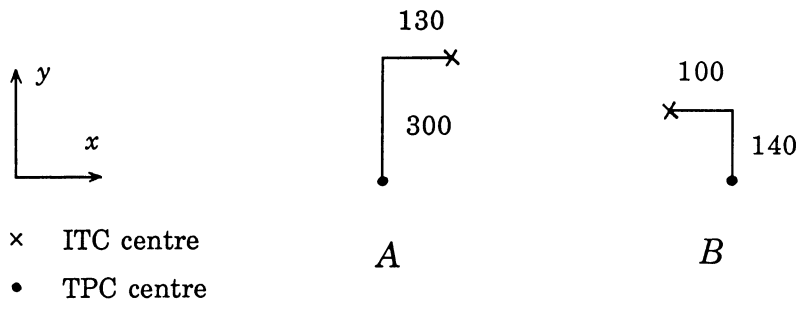


**Figure 6** *Expected offset of ITC from TPC at each end, from target rings [μm]*

Preparations were now made for inserting the ITC into the TPC. A roller system was set up at the $B$-end of the TPC. It consisted of 4 sets of rollers mounted on rails, supported by concrete blocks. Each set had 2 rollers at 45° to the vertical, of adjustable extension. A support pipe of slightly greater length than the ITC assembly and of smaller diameter was laid on the rollers, and—using their adjustments—aligned to the centre of the TPC bore. It was then pushed through to the $A$-end where a further set of rollers was arranged to support it. This pipe was to serve as a support for the ITC during insertion, which otherwise would be supported only at one end, and the resulting sag would make the insertion impossible. A final roller at the $A$-end bore down on the top of the support pipe, to adjust its sag.

The ITC was next lowered onto the rollers, so that they made contact with the support tubes of the chamber, two sets on each tube. See Fig. 7. The chamber was aligned to the TPC bore using the roller adjustments, and the support pipe was bolted to the $A$-end of the chamber assembly. The support pads were removed again, and the survey targets were removed from the $A$-end of the chamber (the end that would be inserted into the TPC) to maximise the available room for insertion.

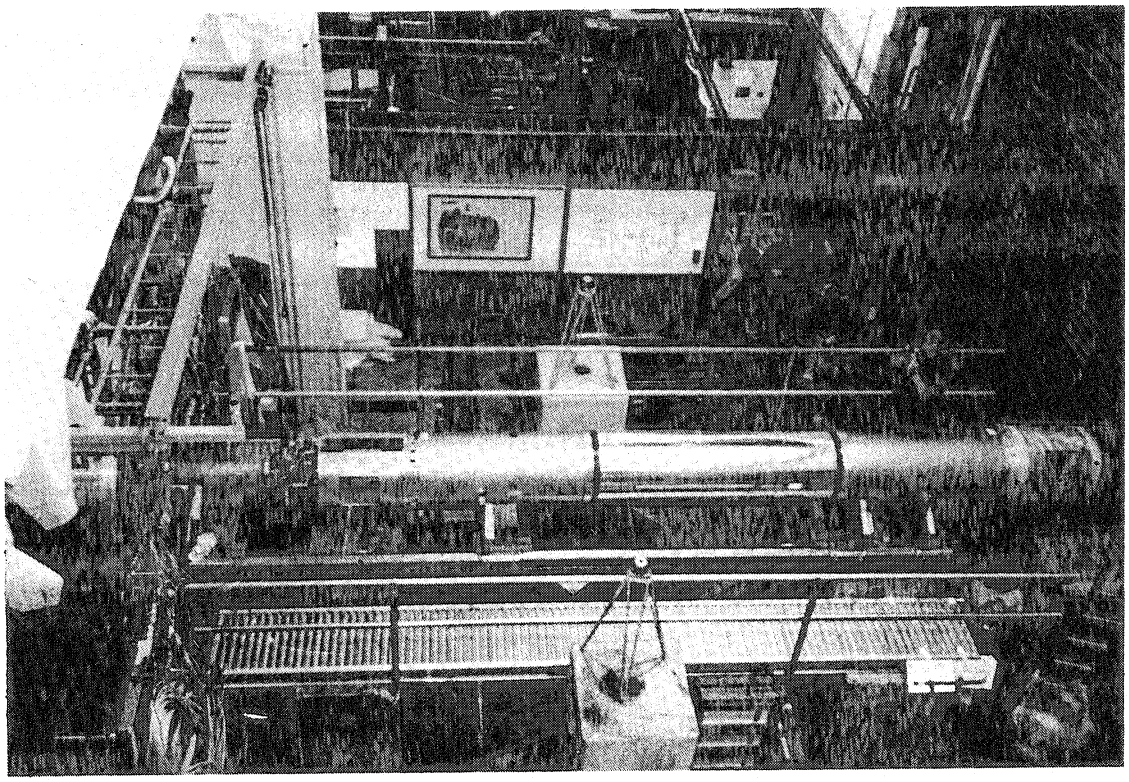

**Figure 7** *The ITC in position on rollers*

# 3 Insertion

The ITC was finally inserted into the TPC on 26th Oct 1988. Two people pushing at the $B$-end were sufficient to move the chamber. A further two people stationed by the $B$-end checked the alignment. They were in contact using an intercom with two people at the $A$-end who checked alignment, looking down the bore of the TPC. At first the chamber was supported on the rear set of rollers on each support tube. As the end of the support tube was reached by this set of rollers, the load was transferred to the front set, which had been moved to the front of the tube. By a sequence of such load transfers the chamber was inserted in short 10–20 cm steps, and after each step it was checked for alignment at both ends before continuing. As the $A$-end support tube disappeared into the TPC, the load was carried by the $B$-end rollers alone. Due to the small amount of free space at the $A$-end side of the TPC, the support pipe would eventually have hit the building wall. For this reason it was constructed out of screw-on segments, and as each segment cleared the rollers it was unscrewed and removed. For the final half-metre or so of insertion, a section of support pipe was attached to the $B$-end, to rest on the rollers when the $B$-end support tube was inside the TPC. Eventually the chamber was fully inserted, the support pads were replaced and the chamber was lowered onto them. Finally the ITC $A$-end survey targets were refitted.

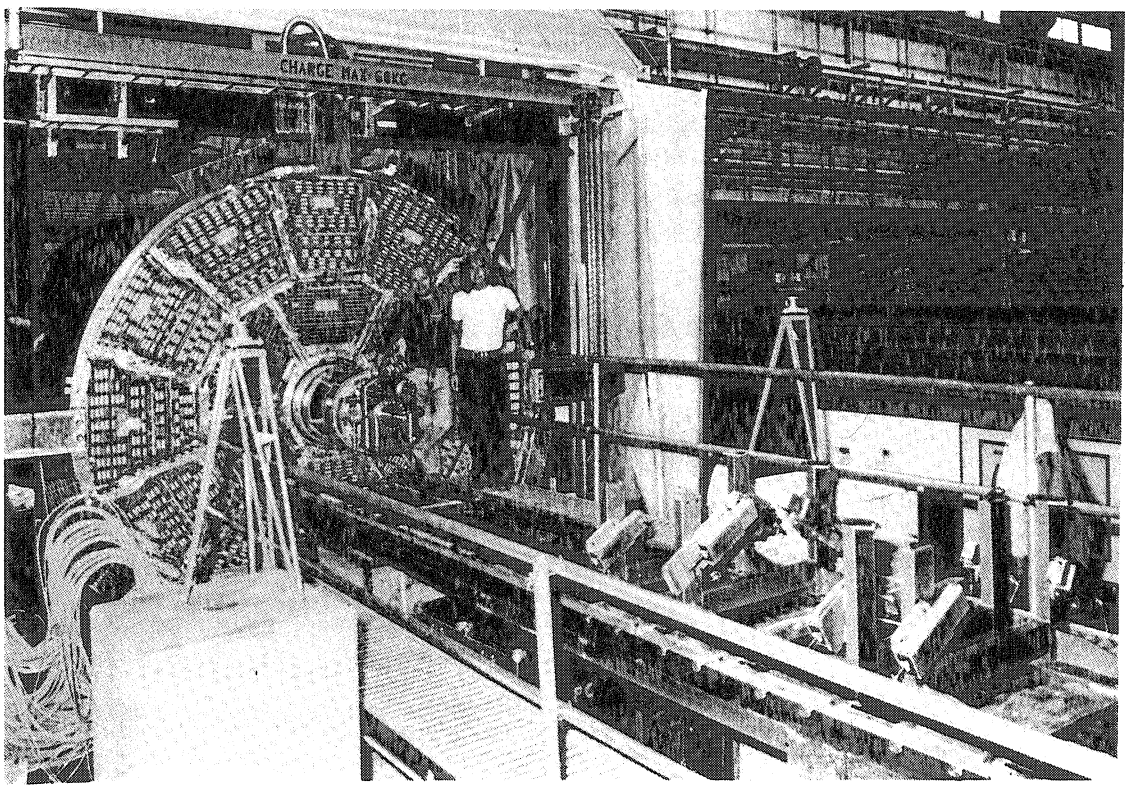

**Figure 8** *The ITC and TPC after assembly*

This whole operation turned out to be rather tense. One of the problems was the large number of people present, with ill-defined rôles. If the operation has to be repeated—for example, after a change of beam-pipe—it would be sensible to limit the number of people involved, and ensure that they have specific tasks. Another problem was that the widest part of the ITC assembly, the support flange, was not the closest object to the people viewing from the $A$-end (due to the attached vacuum pumps), which made judging how close the chamber was to the TPC inner wall a difficult business. It would be easier if, for example, a disc of white card of slightly greater diameter than the support flange was attached to the end of the chamber assembly before insertion.

The ITC–TPC assembly can be seen in Fig. 8, after the insertion had been completed. Also visible in the figure is the roller system at the $B$-end. Further photographs can be found in Ref. 4.

# 4 Survey

Now that the chamber was in position on its support pads, the rotational alignment relative to the TPC had to be adjusted (for the azimuthal angle, $\phi$). The sector targets on a roughly vertical axis were taken to define a reference axis for the measurement of $\phi$, since there were the most targets surveyed for this axis, on the two TPC endfaces. A plot of their $x$ coordinate as a function of $y$ is shown in Fig. 9 (solid points), using the values from Tables 5 and 6 for the two ends. As can be seen, the points lie relatively close to a straight line, indicating a rotation of the TPC from the true vertical. The points have been fit with a straight line, of the form

$$x = \phi_0 y + x'_0 \quad .$$

Defining $\phi$ to be positive if anticlockwise when viewed from the $A$-end, we find

$$\begin{aligned} \phi_0^A &= -1{\cdot}22\,\mathrm{mrad} \\ \phi_0^B &= -1{\cdot}17\,\mathrm{mrad} \quad , \end{aligned}$$

consistent with the same rotation at both ends.

(a) *A*-end

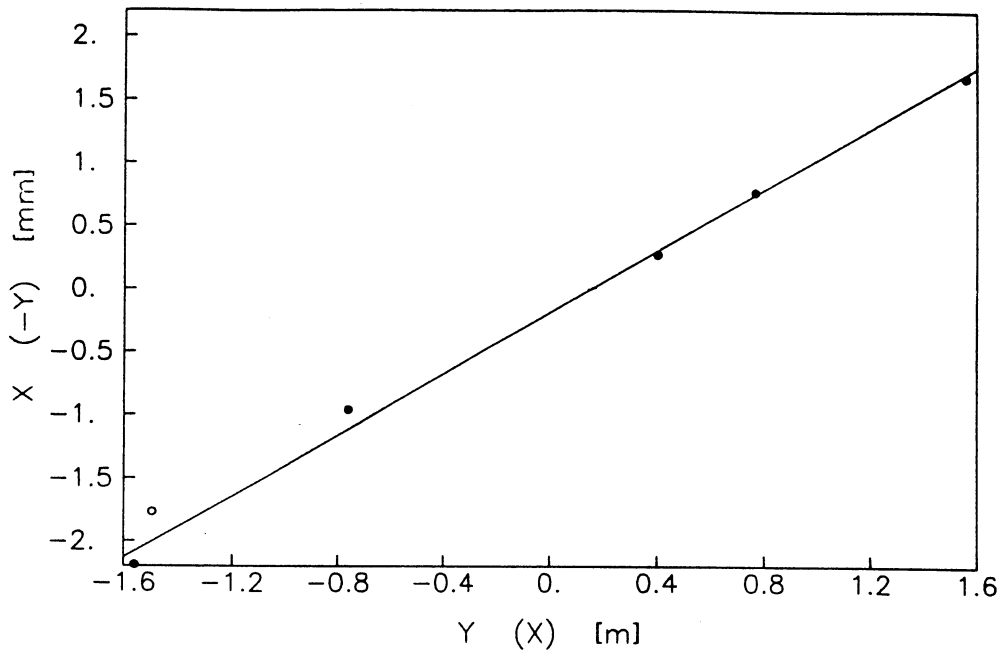


(b) *B*-end

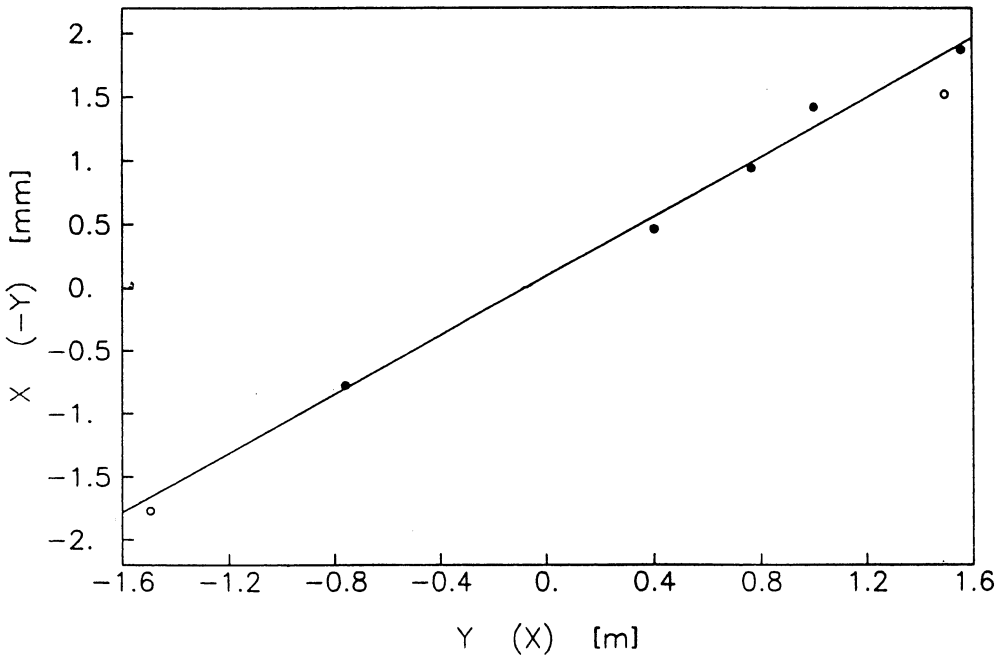


**Figure 9** *The x-coordinate of the TPC survey targets v. y*

For the measurements up to this point triangulation had been used to provide three coordinates for each surveyed target; now a different form of survey was used: a levelling technique. This allows a horizontal plane to be defined, and the vertical offset of targets close to that plane can be measured. The TPC sector targets nearest to the horizontal were used to provide the TPC reference position. These are the targets of sectors 7 and 13 at the $A$-end, and sectors 25 and 31 at the $B$-end. As a check that they give a consistent reference in $\phi$ to that measured with the vertical targets, a plot of $-y$ against $x$ is superimposed on Fig. 9 (open points), and as can be seen, the points are consistent with the same $\phi_0$. For the ITC position, the survey targets nearest to horizontal were used, $SA2$ and $SA4$ at the $A$-end, and $SB2$ and $SB4$ at the $B$-end (see Ref. 1).

First the $B$-end was measured. The raw vertical offsets are given in the first row of Table 8, where the targets are labelled according to their $x$-coordinate. Expressing these offsets relative to the lowest target (at $x = +1{\cdot}5\,\mathrm{m}$, TPC sector 25) leads to the arrangement shown in Fig. 10 (a). This indicates that the rotation of the ITC is $+2310\,\mu\mathrm{m}$ over $600\,\mathrm{mm} = +3{\cdot}85\,\mathrm{mrad}$. The rotation of the ITC relative to the TPC is therefore $+5{\cdot}02\,\mathrm{mrad}$. There is one more effect to be taken into account: the rotation defined by the ITC survey targets (mounted on the support flanges) does not agree exactly with the rotation of the *true* ITC (defined by the wire-flanges, which hold the chamber wires). This difference has, however, been previously determined [1], and the relevant offsets (in $x$ and $y$ as well as $\phi$) are reproduced in Table 9, taken from Ref. 1. Correcting for this effect gives a final rotation of $+6{\cdot}02\,\mathrm{mrad}$ for the ITC relative to the TPC, which is equivalent to $1{\cdot}8\,\mathrm{mm}$ at the outer radius of the ITC.

This was corrected by manually rotating the chamber. The $B$-end was then surveyed again, and it was found the the correction was too great by $0{\cdot}8\,\mathrm{mm}$. After a further attempt, the final values of the raw vertical measurements, for both the $B$- and

| | Target $x$-coordinate [m] | | | |
|---|---|---|---|---|
| End | $-1{\cdot}5$ | $-0{\cdot}3$ | $+0{\cdot}3$ | $+1{\cdot}5$ |
| $B$ | 1·55602 | 1·55334 | 1·55563 | 1·55274 |
| $B$ | 1·55606 | 1·55524 | 1·55374 | 1·55278 |
| $A$ | 0·09647 | 0·09444 | 0·09369 | 0·09276 |

**Table 8** *Heights of survey targets [m]*

| Offset | $A$ | $B$ |
|---|---|---|
| $\Delta x$ | 200 | 50 |
| $\Delta y$ | −530 | 180 |
| $\Delta\phi$ | −130 | −300 |

**Table 9** *Offset of ITC support flanges, from true position [$\mu$m]*

$A$-ends, are given in rows 2 and 3 of Table 8. They correspond to the arrangements shown in Fig. 10 (b) and (c). These indicate a rotation of the ITC relative to the TPC of +0·37 mrad (110 $\mu$m at the outer radius of the ITC) at the $A$-end, and −0·33 mrad (100 $\mu$m at the outer radius of the ITC) at the $B$-end. This suggests a twist of the chamber (plus support tubes) of 0·70 mrad, corresponding to 90 $\mu$m at the outer radius of the ITC wire flange. The error on the levelling measurements is given as $\pm$100 $\mu$m, however, so the twist seen is at the limit of the measurement accuracy. A fibre-glass bracket was fastened at the top of the ITC to prevent any further movement in $\phi$.

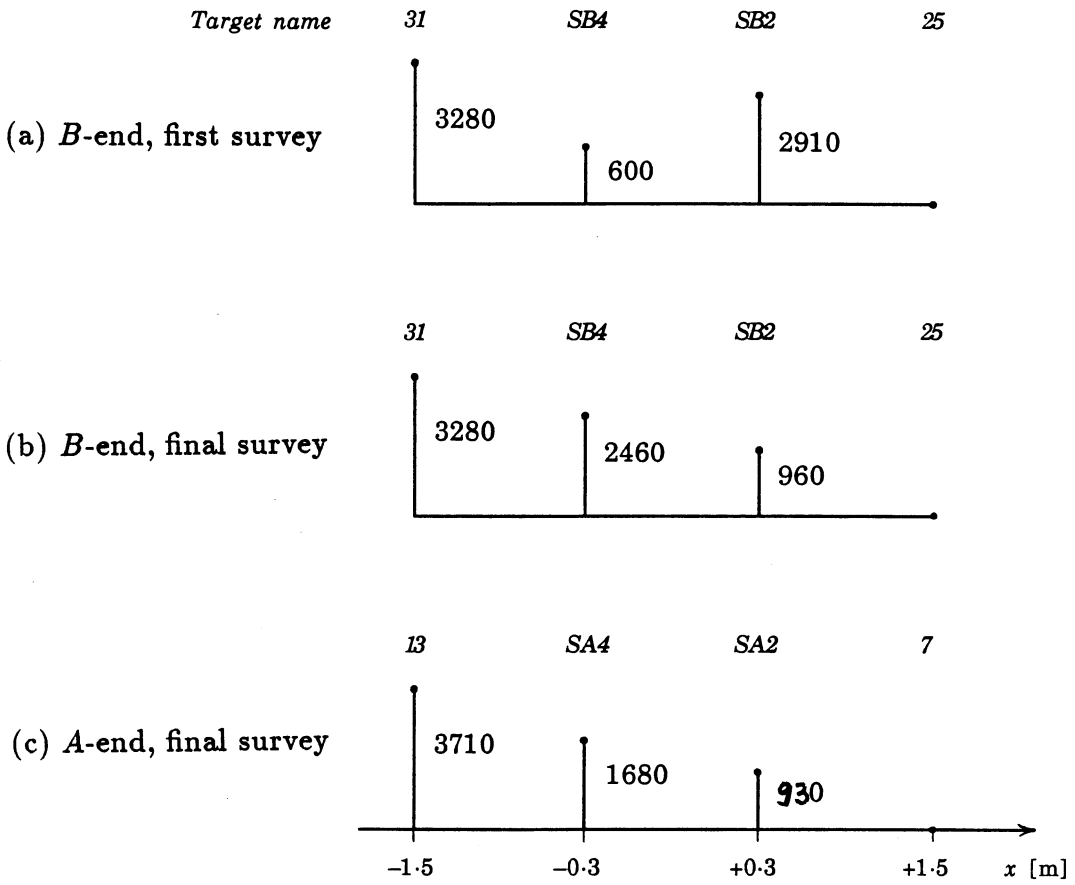


**Figure 10** *Relative heights of survey targets [$\mu$m]*

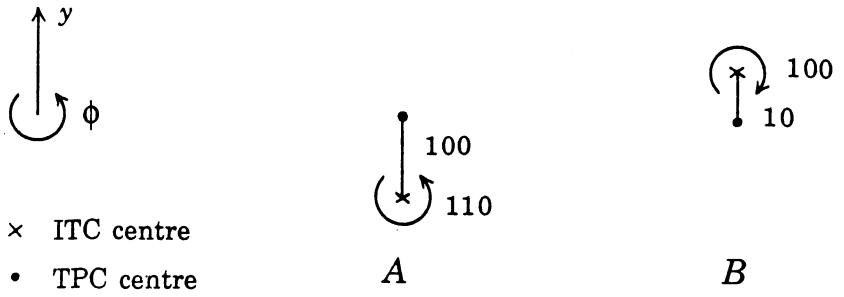


**Figure 11** *Offset of ITC from TPC at each end, from levelling measurements [$\mu$m]*

The levelling measurements may also be used to check the vertical alignment of the ITC to the TPC. From Fig. 10 (c), the centre of the ITC $A$-end support flange (defined using $SA\,2$ and $SA\,4$) is 2400 $\mu$m below the left-hand TPC target, from sector 13. Using the $y$-coordinate of this target relative to the centre of the TPC from Table 5, we find that the centre of the $A$-end support flange is 630 $\mu$m below the TPC centre. Finally, the true axis of the ITC is 530 $\mu$m above the centre of the $A$-end support flange, from Table 9. Thus the ITC axis is 100 $\mu$m above the TPC endface centre, at the $A$-end. A similar calculation for the $B$-end shows that the ITC axis is 10 $\mu$m above the TPC endface centre at the $B$-end. This information is summarized in Fig. 11.

# 5 Conclusions

The ITC was successfully inserted into the TPC on 26th Oct 1988. The use of target rings ensured the accurate alignment of the ITC to the TPC. Results of a survey performed after the assembly indicate that the ITC was aligned vertically and in $\phi$ to the TPC to better than 200 $\mu$m.

The final alignment constants for the ITC relative to the TPC, to be taken from the survey information, will depend on surveys performed when the ITC–TPC assembly is installed in the pit. If the relative alignment has changed, then corrections will be made *in situ*. Finally the reconstruction of cosmic rays will allow more precise alignment of the two detectors.

## Acknowledgements

The surveying was performed by Odile Lemâitre, Corinne Meyer and Julien Veaux of the CERN *SU* division. Derek Miller organized the assembly of the chambers, assisted by Geoff Barber, Dave Clark and Ron Hobbs. Thanks are also due to the members of the TPC group that assisted during the insertion.

## References

[1] R.W. Forty, *Survey of the ITC*, ALEPH–88–83 LAYOUT–88–3

[2] R. Johnson, *TPC Alignment Constants and Coordinate Conventions*, ALEPH–88–135 SOFTWR–88–16

[3] O. Lemâitre, C. Meyer, J. Veaux, *Survey results*, (Oct–Dec 1988)

[4] *ALEPH Times*, No. 9, (Dec 1988)